Dynamic localization and second-order subgrid-scale models in large eddy simulations of channel flow

By W. Cabot

1. Motivation & objectives

The dynamic subgrid-scale (SGS) model (Germano *et al.*, 1991; Lilly, 1992) has been applied successfully in the large eddy simulation (LES) of flows with relatively simple geometry and physics, e.g., in homogeneous flow (Moin, *et al.*, 1991) and in channel flow (Germano *et al.*, 1991; Cabot & Moin, 1993). In these flows a global dynamic coefficient is determined from averages over one or more homogeneous directions, which generally gives well behaved results (i.e., positive eddy viscosities, or, at least, positive net eddy plus molecular viscosities). But for arbitrary, complex geometries, no global homogeneity may exist, precluding this averaging procedure. The dynamic localization (DL) model of Ghosal, Lund & Moin (1993) addresses this problem by fitting *local* dynamic coefficients with a global minimization procedure. However, this model, like all local dynamic SGS models, results in persistent points or regions of negative eddy viscosity that become numerically unstable. Ghosal *et al.* (1993) have proposed to alleviate this problem either (1) by constraining the dynamic coefficient (and eddy viscosity) to be non-negative or (2) by limiting the time that a point can have negative eddy viscosity by evolving an auxiliary equation for the residual SGS kinetic energy k. When k is forced to zero by a persistently negative eddy viscosity, the eddy viscosity also vanishes. Both of these procedures with the DL model were found in homogeneous flow to give stable numerics and to give results in good agreement to those using global averaging and to experiments (Ghosal *et al.*, 1993; Ghosal, this volume). The objective here is to test the DL model in a wall-bounded channel flow for numerical stability and accuracy of results.

Algebraic stress models (cf. Gatski & Speziale, 1993) suggest that the model for the residual SGS Reynolds stress and scalar flux should generally have terms comprising most of the unique products of the resolved strain ($\mathbf{S}$) and rotation ($\mathbf{R}$) tensors with $\mathbf{S}$ and the resolved scalar gradient. The standard dynamic SGS model uses a simple (Smagorinsky) base model for the residual Reynolds stress, which is made proportional to $\mathbf{S}$, and down-gradient base models for residual scalar fluxes; these correspond to the lowest, "first-order" terms in algebraic stress models. Temporal scaling terms in these base models are formed from the magnitude of the resolved strain rate. While this is appropriate for simple shear flows, it may not be appropriate for more complicated flows (relevant to geophysical and astrophysical problems) that include any combination of shear, rotation, buoyancy, etc. On the other hand, the coefficient in the dynamic SGS model readily adjusts itself to different flow conditions and may adequately take account of these effects without the need for more complicated base models. Cabot (1993) has begun to test the

dynamic SGS model in buoyant flows (Rayleigh-Bénard and internally heated convection) with and without buoyancy terms explicitly included in the scaling terms of the base model; no great differences were found in LES results for the different base model scalings. The second objective in this work is to test base models with additional, "second-order" terms (e.g., $\mathbf{S}^2$ and $\mathbf{RS}$ for the residual Reynolds stress). These terms have been found to improve large-scale flow predictions by k-ε models in the presence of rotation and shear (Gatski & Speziale, 1993). Second-order base models will be tested here in the LES of channel flow with and without solid-body rotation and compared with results from the standard first-order base models to determine if there are significant differences or improvements in results that would warrant the added complexity of the second-order base models.

2. Accomplishments

2.1 Dynamic localization subgrid-scale models in channel Ffow

2.1.1 The constrained model

The dynamic localization (DL) model was implemented in a pseudospectral channel flow code (cf. Kim, Moin & Moser, 1987). The procedure was tested using a Smagorinsky base model for the trace-free (*) part of the residual SGS Reynolds stress at the resolved scale (denoted by $\bar{}$),

$$\tau_{ij}^* \equiv (\overline{u_i u_j} - \overline{u}_i \overline{u}_j)^* \simeq -2\nu_t \overline{S}_{ij} = -2C\Delta^2 |\overline{S}| \overline{S}_{ij} \,, \tag{1a}$$

and at a coarser test scale (denoted by $\widehat{\ }$),

$$T_{ij}^* \equiv (\widehat{\overline{u_i u_j}} - \widehat{\overline{u}}_i \widehat{\overline{u}}_j)^* \simeq -2\hat{\nu}_t \widehat{\overline{S}}_{ij} = -2C\hat{\Delta}^2 |\widehat{\overline{S}}| \widehat{\overline{S}}_{ij} \,, \tag{1b}$$

where the *local* coefficient $C(\mathbf{x})$ is constrained to be ≥ 0 to ensure numerical stability (model "DL+"). The strain rate tensor $S_{ij} \equiv (u_{i,j} + u_{j,i})/2$, and its magnitude $|S| \equiv (2S_{ij}S_{ij})^{1/2}$; Δ, $\hat{\Delta}$ are the effective filter widths of the resolved and test fields, defined as some average of the grid spacings in each direction. The coefficient C is solved by the iterative global minimization procedure described by Ghosal *et al.* (1993). By using the coefficient field from the previous time step, only two or three iterations were needed per time step to converge the minimization to acceptable accuracy ($< 1\%$ error in the L^1 norm); most of the computational expense of the procedure results from the many additional filtering operations that are needed.

Also, because the code is pseudospectral, terms involving the spatially varying eddy viscosity must be computed explicitly, unlike the terms with uniform molecular viscosity, which are computed implicitly. For a plane in the channel, the locally computed dynamic coefficient has extrema about 10 times the plane average. Even in low Reynolds number simulations, this causes the time step to be limited to several times lower than the limit from the convective CFL number.

A low Reynolds number simulation (with friction Reynolds number $Re_\tau \equiv u_\tau \delta/\nu$ = 180, where δ is the channel half-width and the friction velocity $u_\tau = |\nu dU/dy|^{1/2}$

at the walls for mean streamwise velocity U and wall-normal direction y) was performed for a channel with streamwise, wall-normal, and spanwise dimensions of $4\pi \times 2 \times 4\pi/3$ (in units of δ) on a $32 \times 65 \times 32$ grid. Filtering and dynamic minimization was performed only in homogeneous horizontal planes. A localized real-space ("tophat") filter was used that employed a trapezoidal integration over adjacent points. The effective ratio of test to resolved field filter width $\widehat{\Delta}/\Delta$ was taken to be 2 in these simulations, although T. Lund (private communication) later showed that the correct (unidirectional) filter width ratio should be $\sqrt{6}$ for trapezoidal integration (but 2 for integration with Simpson's rule). The issue of how one properly combines the unidirectional filter width ratios into the effective filter width ratios for non-uniform grids (e.g., Scotti, Meneveau & Lilly, 1993) or for two-dimensional filtering is still not settled.

As found in simulations of homogeneous flow, constraining the dynamic coefficient to be non-negative, while stabilizing the numerics, causes the mean eddy viscosity $\langle \nu_t \rangle$ from the DL+ model to be about twice that found from the same base model (Eq. [1]) with plane averaging (model "DA1"). (In the interior, $\langle \nu_t \rangle$ is found to be about half the molecular viscosity ν in the DA1 model.) However, the final large-scale statistics (mean streamwise velocity U, and resolved Reynolds stress $\langle -\overline{u}\,\overline{v} \rangle$ and velocity fluctuation intensities $u_{i\,\mathrm{rms}}$) are almost indistinguishable between the two cases (see Fig. 1) and are in good agreement with the well resolved direct numerical simulation (DNS) of Kim *et al.* (1987) computed on a $128 \times 129 \times 128$ grid. The insensitivity in this flow to the SGS model is also a consequence of the small contribution to the total $\langle uv \rangle$ by the residual SGS component (about 20% very near the wall to $< 10\%$ in the interior). But note in Figure 1 that a "coarse DNS" (computed at the LES resolution with *no* SGS model) gives quite poor results for U, which is seen to be about 15% lower than in the well resolved DNS, and equally poor results for resolved turbulence intensities and Reynolds stress are obtained when compared with filtered DNS results. Note that, in general, when ν_t is increased in plane-averaged models, U increases and u_{rms} decreases.

2.1.2 Auxiliary one-equation models

Retaining negative local values of the dynamic coefficient C requires that their persistence be limited by use of an auxiliary equation for the residual SGS kinetic energy $k \equiv \tau_{ii}/2$. When persistent negative eddy viscosities use up all the local SGS kinetic energy, one wants the eddy viscosity to turn off. The base model for the residual SGS Reynolds stress is now given in terms of k as

$$\tau_{ij}^* \simeq -2\nu_t \overline{S}_{ij} = -2C\Delta k^{1/2} \overline{S}_{ij}\,, \tag{2a}$$

$$T_{ij}^* \simeq -2\widehat{\nu}_t \widehat{\overline{S}}_{ij} = -2C\widehat{\Delta} K^{1/2} \widehat{\overline{S}}_{ij}\,, \tag{2b}$$

where $K \equiv T_{ii}/2$. The governing equations for the k and K are

$$k_{,t} + (k\overline{u}_i)_{,i} = -\overline{S}_{ij}\tau_{ij}^* - d_{i,i} - \varepsilon + \nu k_{,ii}\,, \tag{3a}$$

$$K_{,t} + (K\widehat{\overline{u}}_i)_{,i} = -\widehat{\overline{S}}_{ij} T_{ij}^* - D_{i,i} - E + \nu K_{,ii}\,, \tag{3b}$$

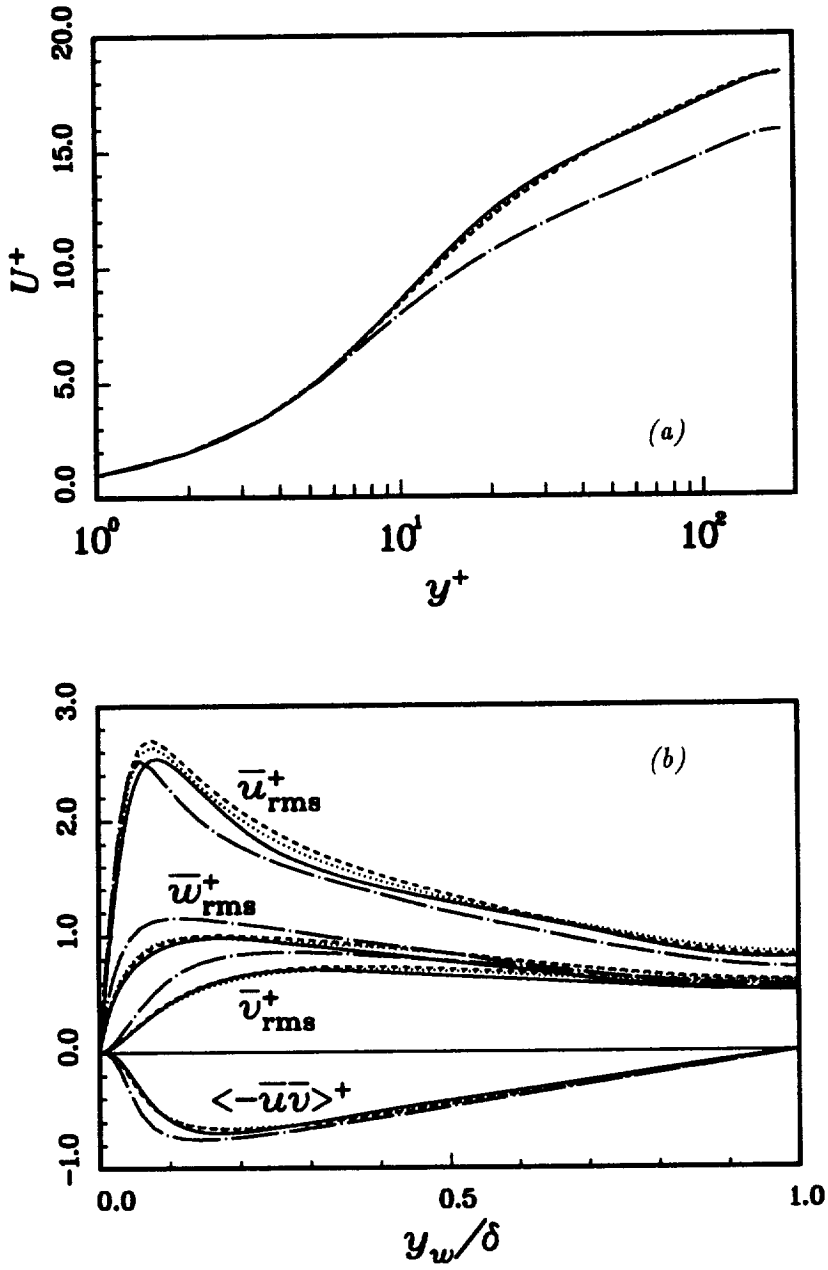

FIGURE 1. *(a)* Mean streamwise velocity as a function of distance from the wall y_w (in wall units: $U^+ = U/u_\tau$, $y^+ = y_w u_\tau/\nu$), and *(b)* resolved rms velocity intensities and Reynolds stress for (——) DNS (Kim *et al.*, 1987), (----) LES with the DA1 model, (—·—) coarse DNS, and (·····) LES with the DL+ model. The DNS data are filtered in *(b)*. The first three curves are nearly indistinguishable except for $u_{\rm rms}$ in *(b)*.

where the residual SGS dissipations,

$$\varepsilon = \nu(\overline{u_{i,j}u}_{i,j} - \overline{u}_{i,j}\overline{u}_{i,j}) \simeq C_e k^{3/2}/\Delta\,, \tag{4a}$$

$$E = \nu(\widehat{\overline{u_{i,j}u}}_{i,j} - \widehat{\overline{u}}_{i,j}\widehat{\overline{u}}_{i,j}) \simeq C_e K^{3/2}/\widehat{\Delta}\,, \tag{4b}$$

and the residual SGS diffusive fluxes,

$$d_i = -\overline{(p + u_j u_j/2)u}_i + (\overline{p} + \overline{u}_j\overline{u}_j/2 + 5k/3)\overline{u}_i + \overline{u}_j\tau^*_{ji} \simeq C_d\Delta k^{1/2}k_{,i}\,, \tag{5a}$$

$$D_i = -\widehat{\overline{(p + u_j u_j/2)u}}_i + (\widehat{\overline{p}} + \widehat{\overline{u}}_j\widehat{\overline{u}}_j/2 + 5K/3)\widehat{\overline{u}}_i + \widehat{\overline{u}}_j T^*_{ji} \simeq C_d\widehat{\Delta}K^{1/2}K_{,i}\,, \tag{5b}$$

are modeled by analogy with standard k-ε models for large scales. In general, the DL procedure is used to determine the local values of C, C_d, and C_e by globally minimizing the residuals of the computable quantities $\mathcal{L}_{ij} \equiv T_{ij} - \widehat{\tau}_{ij}$, $D_i - \widehat{d}_i$, and $E - \widehat{\varepsilon}$ with their model expressions in equations (3–5) above. In this formulation, the pressure field $\overline{p}$ must be computed and saved at each time step.

An alternative formulation is given by Ghosal *et al.* (1993), who write from equations (3) and (5)

$$(D_j - \widehat{d}_j)_{,j} = [(\mathcal{L}_{ii,t} + \widehat{\overline{u}}_j\mathcal{L}_{ii,j} - \nu\mathcal{L}_{ii,jj})/2 + \widehat{\overline{S}}_{ij}T^*_{ij} - \widehat{\overline{S}_{ij}\tau^*_{ij}}] + (K\widehat{\overline{u}}_j - \widehat{k\overline{u}}_j)_{,j}\,. \tag{6}$$

The non-diffusive terms in the square brackets are incorporated in the expression for $E - \widehat{\varepsilon}$, and only the last, remaining terms are used for $D_j - \widehat{d}_j$. In this formulation, the terms in (6) with $\mathcal{L}_{ii} = 2(K - \widehat{k})$ must be computed and saved at each time step. Note that the dynamic coefficients from either formulation are Galilean invariant. At this time it is not known how this rearrangement of terms affects the model coefficients in channel flow applications. However, S. Ghosal (private communication) has pointed out that the formulation of the residual dissipation used here, unlike that of Ghosal *et al.* (1993), has the unphysical property of vanishing in the high Reynolds number limit ($\nu \to 0$).

A low Reynolds number LES (with the same setup and parameters as described in the previous subsection) was initiated using this ("DLk") model. All terms in (3a), except the molecular viscosity term, are integrated explicitly in the numerical code. For real space filters, k and ε are positive semi-definite by definition. In the DL procedure, C_e is therefore constrained to be non-negative. For points where diffusion occasionally causes k to become negative, an artificial source term is substituted for the right-hand side of (3a) to drive the point to zero at the next time step, and the eddy viscosity is taken to be zero. Although there is no direct constraint on the sign of C_d, in most cases it is also constrained to be non-negative in order to ensure the realizability of k. However, its unconstrained interior values were found to be almost 50% negative with no preferred sign in the mean, so that the mean constrained diffusive eddy viscosity $\langle C_d\Delta k^{1/2}\rangle \sim 20\nu$ is probably greatly overestimated. Near the wall, the unconstrained values of C_d are finite, but small,

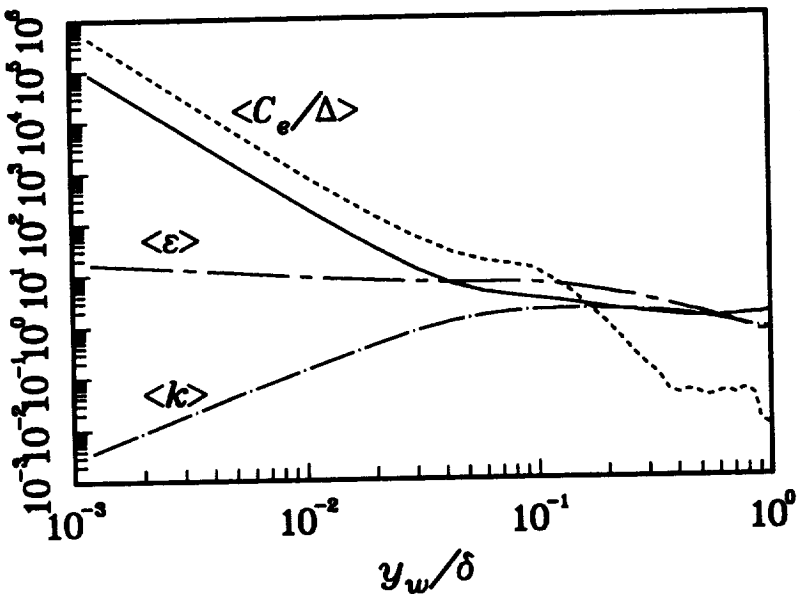

FIGURE 2. Near-wall behavior of the mean dynamic dissipation coefficient for the k-equation in channel flow using (——) Δ_e and (----) Δ as the effective filter width. Also the mean residual SGS dissipation rate, $\langle\varepsilon\rangle = \langle C_e k^{3/2}/\Delta_e\rangle$, and $\langle k\rangle$.

and almost entirely positive. It will be interesting to compare the results using Ghosal *et al.*'s (1993) alternative expression for C_d.

At first, the filter width ratios $\widehat{\Delta}/\Delta$ for equations (2), (4), and (5) were assumed to be all the same. It was found, however, that constrained C_e from the DLk model became largely (90%) zero near centerline in the flow, giving very small values of $\langle\varepsilon\rangle$ there. An alternative definition for effective filter width was tried for C_e (by analogy with wavenumbers) as the harmonic mean of the unidirectional filter widths, $\Delta_e^{-2} = \sum_i \Delta_i^{-2}$; this causes the effective filter width ratio $\widehat{\Delta}_e/\Delta_e$ to be nearly unity (due to the small grid spacing in the wall-normal direction, for which no explicit filtering occurs) instead of 2. This results in very few zero points and a mean value of C_e that varies smoothly throughout the channel. A comparison of C_e/Δ and C_e/Δ_e is shown in Figure 2. In both cases, $C_e/\Delta_{(e)}$ approaches the wall as nearly y_w^{-3}, where y_w is the normal distance from the wall. This nearly balances the approximate (but slightly sub-)y_w^3 behavior of $k^{3/2}$ near the wall so that $\langle\varepsilon\rangle$ rises relatively slowly near the wall. Note that the near-y_w^2 behavior of k found at the wall is not guaranteed by the differential equations, which only require that k vanish linearly at the walls.

The extremely rapid rise of C_e/Δ_e at the wall leads to severe time step constraints since the dissipation term is integrated explicitly and the CFL number $(C_e k^{1/2}/\Delta_e)_{\max}\delta t$ goes as y_w^{-2} near the wall. The time step δt must be reduced by more than 100 times that used for the standard DA1 model. This makes the use

of the DLk model prohibitively expensive unless one can perform the integration of the ε-term in (3a) implicitly. This can be accomplished with a finite-difference channel code, which is presently being developed.

In fact, statistics have not been generated for this LES due to its great computational expense. However, instantaneous large-scale statistics look quite good (see Fig. 3) for this model. The mean eddy viscosity was found to be about twice that from the plane-averaged dynamic SGS model. Nevertheless, its prediction of the near-wall streamwise velocity fluctuation intensity (Fig. 3b) appears to be somewhat better than from the plane-averaged SGS model. The value of the residual SGS kinetic energy k can be compared with that computed from the residual of a well resolved DNS field (Kim *et al.*, 1987) when filtered to the LES scale. This is shown in Figure 4, where it is seen that k from the DLk model is generally about twice the actual value in the interior, but dips inappropriately near the wall below DNS values. Note, however, that neither is the SGS model expected to give an accurate prediction of k, nor should the incompressible LES be particularly sensitive to the exact value of k, since it acts only as a scaling term in the eddy viscosity.

Another version of the one-equation DL model has been considered in which $q = (\tau_{ii})^{1/2} = (2k)^{1/2}$ is used in the auxiliary equation. This ("DLq") model was originally proposed by Cabot (1993) to ensure the exact $k \propto y_w^2$ behavior near the wall. (It has been found, meanwhile, that this behavior is approximated reasonably well using the DLk model.) Equation (3a) governing k becomes

$$q[q_{,t} + (q\overline{u}_i)_{,i}] = 2c\Delta q|\overline{S}|^2 - q[(c_d\Delta q + \nu)q_{,i}]_{,i} + (c_d\Delta q + \nu)(q_{,i}q_{,i}) - \varepsilon\,, \quad (7)$$

where factors of $2^{1/2}$ have been absorbed in the new dynamic coefficients, c and c_d. One cannot divide through by q in (7) because of the term $\nu(q_{,i}q_{,i})$. However, the combination $\varepsilon' = \varepsilon - \nu(q_{,i}q_{,i})$ vanishes as y_w^2 at the wall, so that ε'/q vanished linearly there and can be modeled by $c_\epsilon q^2/\Delta_\epsilon$. Dividing (7) through by q now gives

$$q_{,t} + (q\overline{u}_i)_{,i} = 2c\Delta|\overline{S}|^2 - [(c_d\Delta q + \nu)q_{,i}]_{,i} + c_d\Delta(q_{,i}q_{,i}) - c_\epsilon q^2/\Delta_\epsilon\,. \quad (8)$$

While this equation is good in exhibiting no extreme near-wall behavior in any of its terms and guaranteeing the right wall behavior of k, it also presents some problems, mathematically and in implementation. When $q \to 0^+$, the first term on the right-hand side of (8) can remain finite (positive or negative) whereas it vanishes in (3a). This mathematical point still needs to be resolved.

Determining the coefficient c_ϵ from $\varepsilon' = \varepsilon - \nu(q_{,i}q_{,i})$ with the DL procedure has proved unsuccessful because ε (depending on $\overline{u}_i$) and the term in q (an independent variable) do not precisely balance near the wall, causing $c_\epsilon/\Delta_\epsilon \to y_w^{-3}$ again, instead of y_w^{-1}. A suitable proxy to ε' for computing c_ϵ with both the right wall and interior behavior has not been found. A low Reynolds number LES was performed with completely *ad hoc* models of $c_d\Delta = \max(0.032\Delta_d, 0.4\nu/u_\tau)$ and $c_\epsilon/\Delta_\epsilon = 0.4/\Delta_d$, where $\Delta_d^{-1} = \Delta^{-1} + 0.4y_w^{-1}$. The choice of numerical coefficients can be chosen to give fair agreement with $k = q^2/2$ computed from the DNS; in Figure 4, it is seen that this particular guess gave values of k about half those from DNS. The

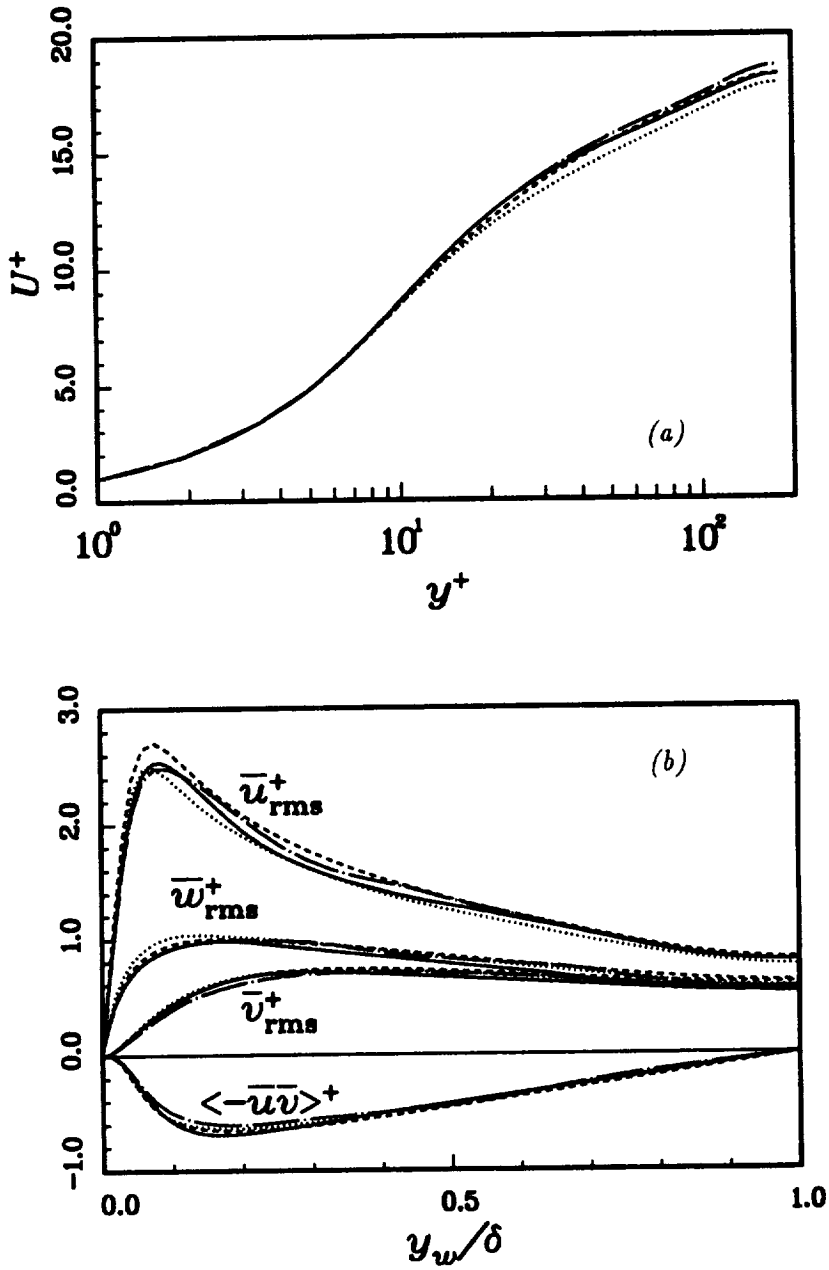

FIGURE 3. *(a)* Mean streamwise velocity as a function of distance from the wall (in wall units), and *(b)* resolved rms velocity intensities and Reynolds stress for (——) DNS (Kim *et al.*, 1987), (- - - -) LES with the DA1 model, (—·—) LES with the DLk model (from an instantaneous field), and (·····) LES with the (*ad hoc*) DLq model. The DNS data are filtered in *(b)*.

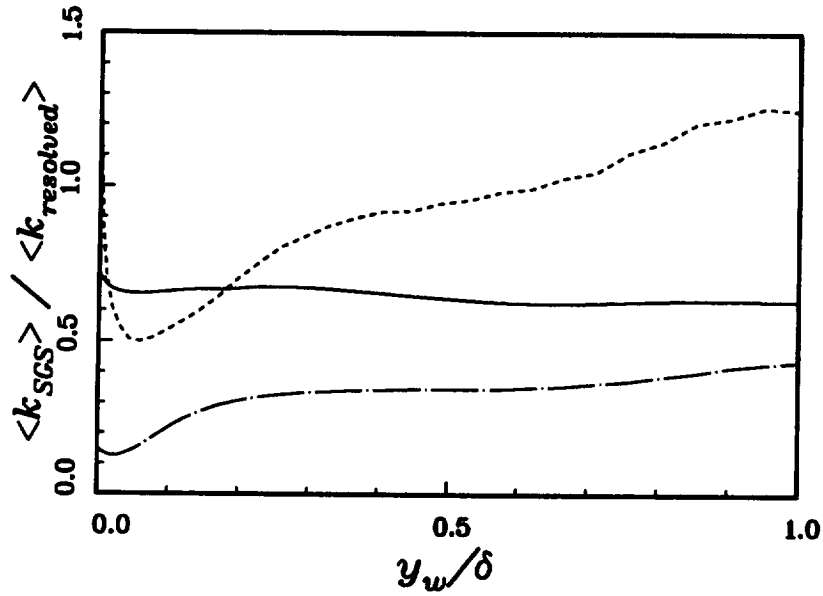

FIGURE 4. The ratio of mean residual SGS kinetic energy to mean resolved kinetic energy computed from (———) DNS, and predicted by (- - - -) the DLk model and (—·—) the *ad hoc* DLq model.

inappropriate dip near the wall also generally occurs for q as it did for k from the DLk model. The simulation was found to be numerically stable and to give about as good agreement with the DNS results as with other SGS models (see Fig. 3). The mean eddy viscosity is found to be slightly lower than from the DLk model, about 80% larger than from the plane-averaged DA1 model.

2.2 Second-order dynamic subgrid-scale models in channel flow

In LES of channel flow with the plane-averaged dynamic SGS model, a second-order base model ("DA2") has been used instead of equation (1) (model "DA1"), having the form

$$\tau_{ij} \simeq -2C_1\Delta^2|\overline{S}|\overline{S}_{ij} + 2C_2\Delta^2\left[\overline{A}_{ik}\overline{S}_{kj} + \overline{A}_{jk}\overline{S}_{ki} - 2\overline{S}_{ij}\mathrm{Tr}(\overline{\mathbf{S}}^3)/\mathrm{Tr}(\overline{\mathbf{S}}^2)\right], \quad (9)$$

and for the residual SGS flux h_i for a passive scalar θ,

$$h_i = \overline{\theta u_i} - \overline{\theta}\,\overline{u}_i \simeq -C_{\theta 1}\Delta^2|\overline{S}|\overline{\theta}_{,i} + 2C_{\theta 2}\Delta^2\left[\overline{A}_{ik}\overline{\theta}_{,k} - \overline{\theta}_{,i}(\nabla\overline{\theta}\cdot\overline{\mathbf{S}}\cdot\nabla\overline{\theta})/(\nabla\overline{\theta}\cdot\nabla\overline{\theta})\right], \quad (10)$$

The tensor A_{ij} is defined

$$A_{ij} \equiv S_{ij} + a_1 R_{ij}, \quad R_{ij} \equiv (u_{i,j} - u_{j,i})/2 - 2\Omega_k a_2 \epsilon_{ijk}, \quad (11)$$

where Ω_k is the system rotation. The lattermost terms in the square brackets in (9) and (10) are included to make the second terms in the model orthogonal to the

first and hence dissipation-free. In practice, the trace is also generally subtracted from (9). This general form is suggested by lowest-order solutions of algebraic stress models (cf. Gatski & Speziale, 1993). The prescribed constants, a_1 and a_2, depend on one's favorite model coefficients; e.g., for the second-order model derived by Gatski & Speziale, $a_1 \approx 1$–3 and $a_2 \approx 1$–2 for commonly used k-ε model constants. This type of large-scale Reynolds stress model has been shown to perform well in flows with rapid solid-body rotation and shear (Speziale, Sarkar & Gatski, 1991).

In initial tests, the more general second-order model was used for (9), in which strain-strain terms ($\mathbf{S}^2$) and rotation-strain terms (**RS**) are kept separate in the dynamic procedure,

$$\begin{aligned}\tau_{ij} \simeq -2C_1\Delta^2|\overline{S}|\overline{S}_{ij} + 2C_2\Delta^2(\overline{R}_{ik}\overline{S}_{kj} - \overline{S}_{ik}\overline{R}_{kj}) \\ + 2C_3\Delta^2\left[2\overline{S}_{ik}\overline{S}_{kj} - 2\overline{S}_{ij}\mathrm{Tr}(\overline{\mathbf{S}}^3)/\mathrm{Tr}(\overline{\mathbf{S}}^2)\right].\end{aligned} \tag{12}$$

It is found that C_3 predicted by the dynamic procedure in channel flow (with $\Omega_k = 0$) is typically about half C_2 and comparable to C_1 (see Fig. 5a), suggesting that the **RS** term may be more important than the $\mathbf{S}^2$ term. Meneveau, Lund & Moin (1992) and Lund & Novikov (1993) also found that, of all the unique products of **S** and **R** (including **S** by itself), the **RS** term was the most highly correlated with τ_{ij} computed from DNS channel flow fields. Another interesting note is that these second-order base models for τ_{ij} in either (9) or (12) *with the trace retained* and for h_i in (10) give the correct (no-slip, fixed scalar) near-wall behavior for *all* of their components (since $C_1\Delta^2, C_{\theta 1}\Delta^2 \propto y_w^3$ but $C_{2,3}\Delta^2, C_{\theta 2}\Delta^2 \propto y_w^2$), which was not the case using only the first terms. The trace of either (9) or (12) also returns the model for the residual SGS kinetic energy used by Moin *et al.* (1991) for LES of compressible flow.

The simultaneous solution of three coefficients in (12) is much more expensive than the two in (9) because many more filtering operations need to be performed, so it was decided to use (9) and (10) in the actual LES of low Reynolds number channel flow (with the same setup and parameters described in the previous subsection). The constants a_1 and a_2 were simply taken as unity (even though $a_1 \approx 2$ is suggested by Fig. 5a). The values of the coefficients returned by the dynamic procedure are shown in Figure 5b: in the interior of the channel we see that $C_2 \approx 2C_1$ and that $C_{\theta 2} \approx C_{\theta 1} \approx C_2$ for $Pr = 0.71$. Large-scale statistics from the LES of channel flow using the DA2 model are compared in Figure 6 with those from LES using the DA1 model and from DNS. The mean eddy viscosity from the DA2 model ($\langle C_1\Delta^2|\overline{S}|\rangle$) is found to be nearly the same as that from the DA1 model (about half that of molecular in the interior). And there is not a great deal of difference between the LES results using first- or second-order SGS base models, except that the agreement of resolved u_{rms} (and thus the resolved kinetic energy) with that from the DNS is somewhat better for the second-order base model, while the mean streamwise velocity is slightly lower like the results using the DLq model (cf. Fig. 3).

The DA2 model was then tested in LES of channel flow rotating about its spanwise axis, which stabilizes the upper wall and destabilizes the lower wall (cf. review by

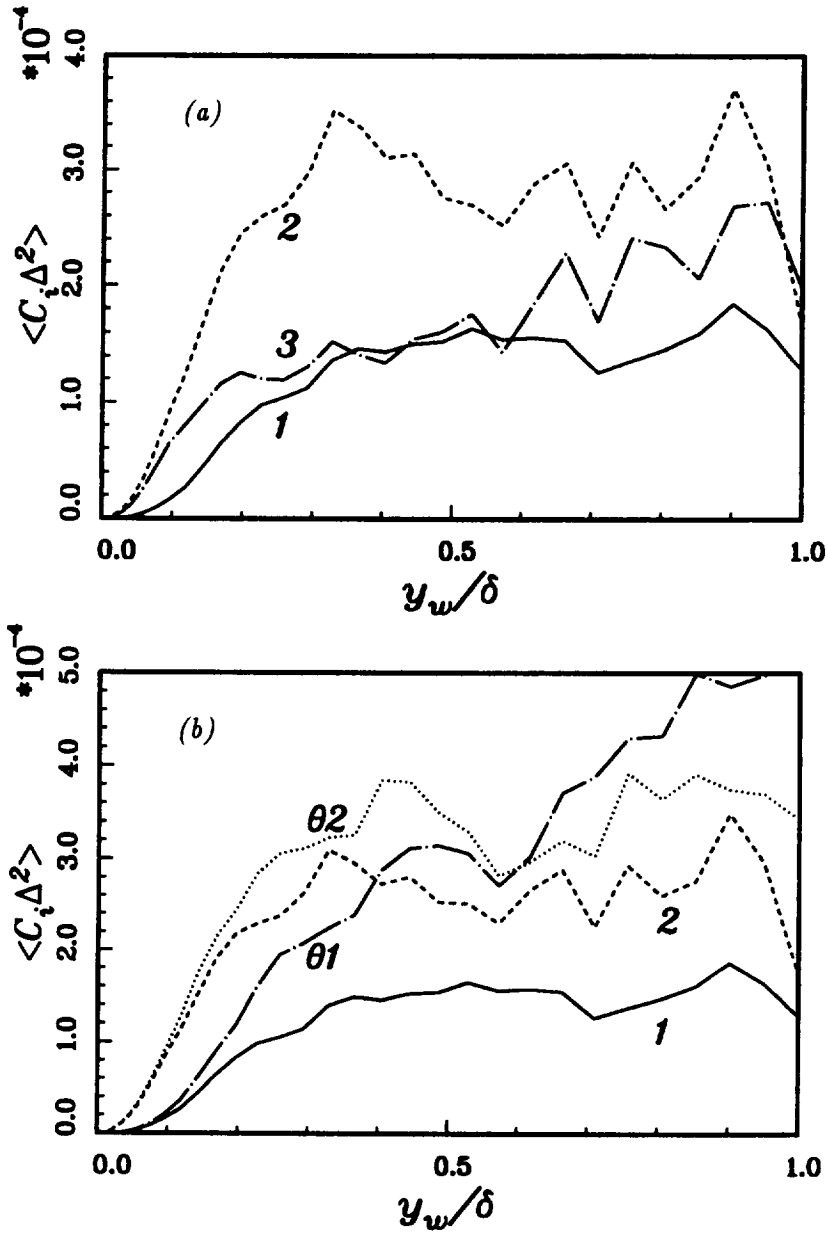

FIGURE 5. Mean dynamic coefficients in channel flow for the second-order base model *(a)* in Eq. (12), and *(b)* in Eqs. (9) and (10).

Moin & Jimenéz, 1993). Again, the standard low Reynolds number case was used (corresponding to a mass-flux Reynolds number $Re_m \equiv 2U_m\delta/\nu \equiv \int_{-\delta}^{\delta} U dy/\nu \approx 5,400$) and for a higher Reynolds number ($Re_m \approx 12,000$) in a $3\pi \times 2 \times \pi$ box (in units of δ). The rotation rates in mass-flux units were $Ro_m \equiv 2\Omega\delta/U_m \approx 0.21$. A

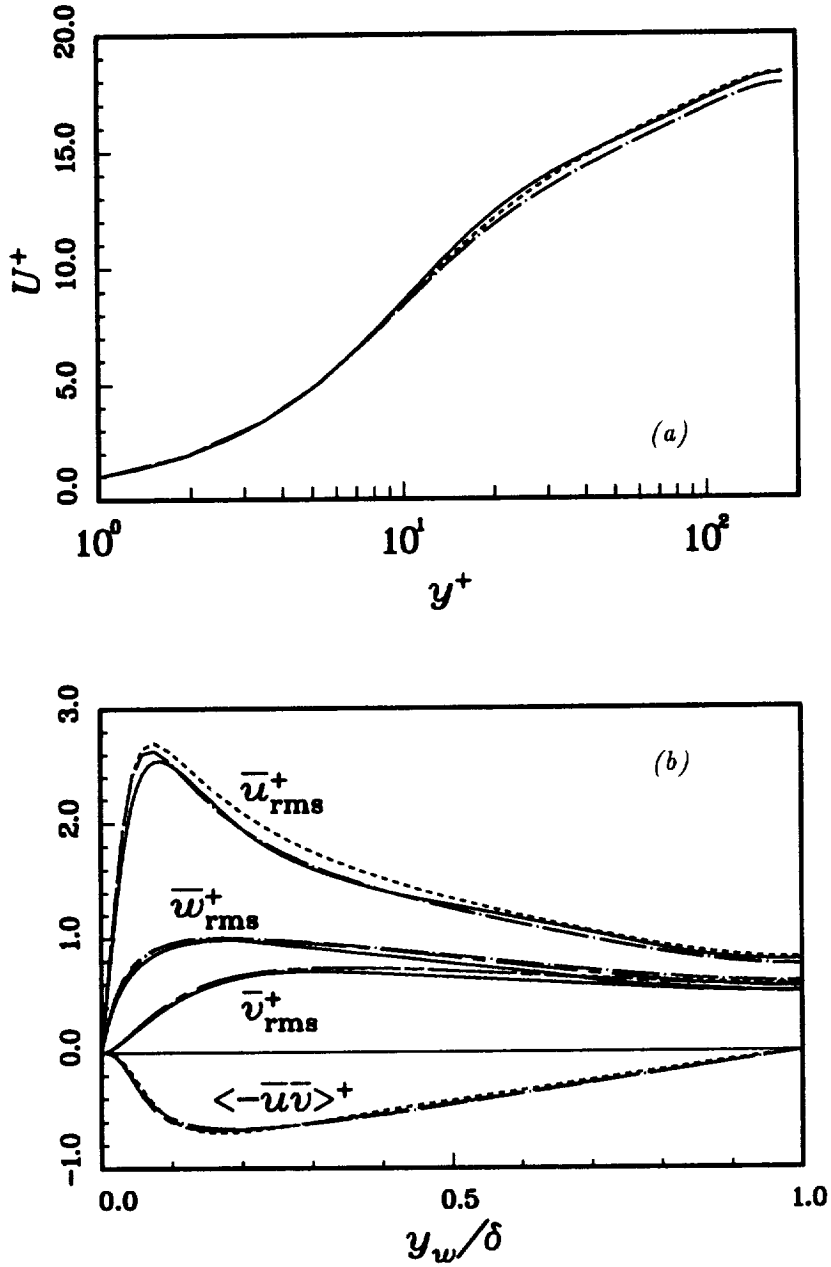

FIGURE 6. *(a)* Mean streamwise velocity as a function of distance from the wall (in wall units), and *(b)* resolved rms velocity intensities and Reynolds stress for (——) DNS (Kim *et al.*, 1987), and for LES with (----) the DA1 model and (—·—) the DA2 model. The DNS data are filtered in *(b)*.

Case	SGS model	$\widehat{\Delta}/\Delta$	Re_m	Ro_m	$u_{\tau 1}/u_\tau$	$u_{\tau 2}/u_\tau$
1	1st order (DA1)	2	5,443	0.217	1.19	0.76
2	2nd order (DA2)	2	5,432	0.218	1.19	0.76
3	1st order (DA1)	2	12,150	0.202	1.16	0.81
4	2nd order (DA2)	2	12,035	0.204	1.15	0.82
5	2nd order (DA2)	$\sqrt{6}$	11,685	0.210	1.14	0.83

TABLE 1. LES of rotating channel flow for different SGS base models: $u_{\tau 1}$ and $u_{\tau 2}$ are the friction speeds at the upper and lower walls, and $u_\tau^2 = (u_{\tau 1}^2 + u_{\tau 2}^2)/2$.

better resolved LES at the higher Re_m was performed in a $4\pi \times 2 \times \pi$ box on a $48 \times 65 \times 32$ grid. This LES also used the correct effective filter width ratio of $\sqrt{6}$ for physical space filtering with integration by trapezoidal rule, instead of the value of 2 used in the rest of LES reported here. It did not give appreciably different results. The parameters and resulting asymmetry of the friction speeds measured at the two walls are summarized in Table 1. The results agree quite well with LES results of Squires & Piomelli (1994), who used the standard DA1 model. The asymmetry in the friction speeds induced by the rotation is seen to be almost independent of Re_m, although the overall asymmetry in the mean streamwise velocity profiles (Fig. 7a) is a little more pronounced. There is again virtually no differences in large-scale statistics using the DA1 as opposed to the DA2 models. About the only noticeable difference is in the shape of the mean residual SGS Reynolds stress $\langle \tau_{12} \rangle$ (Fig. 7b): for the DA2 models it is larger in the interior of the flow and less concentrated at the lower, rotationally unstable wall than for the DA1 models. However, $\langle \tau_{12} \rangle$ is still an order of magnitude less than the resolved Reynolds stress here, which is in part why the large-scale flow is rather insensitive to these differences.

3. Future plans

The dynamic localization model will be implemented in a finite-difference channel code. Terms in the auxiliary governing equation for the residual SGS kinetic energy that are large in near-wall region will be integrated implicitly with much larger time steps than possible with the explicit integration required in the pseudospectral code. This will allow us to generate steady-state statistics in channel flow LES and perform more extensive tests for this local dynamic SGS model.

Second-order base models for the plane-averaged dynamic SGS model will be tested in the LES of uniformly and differentially rotating thermal convection including additional buoyancy terms as suggested by algebraic stress models (cf. Schumann, 1991), and the results will be compared with previous DNS results (Cabot *et al.*, 1990; Cabot & Pollack, 1992) and those from LES performed with the first-order (Smagorinsky) base model. We will again attempt to determined whether the added complexity and computational expense of higher-order, more sophisticated base models is needed in more physically complicated flows or, as it appears so far, that the self-adjusting nature of the dynamic procedure allows one to obtain the same result with simple, relatively inexpensive base models.

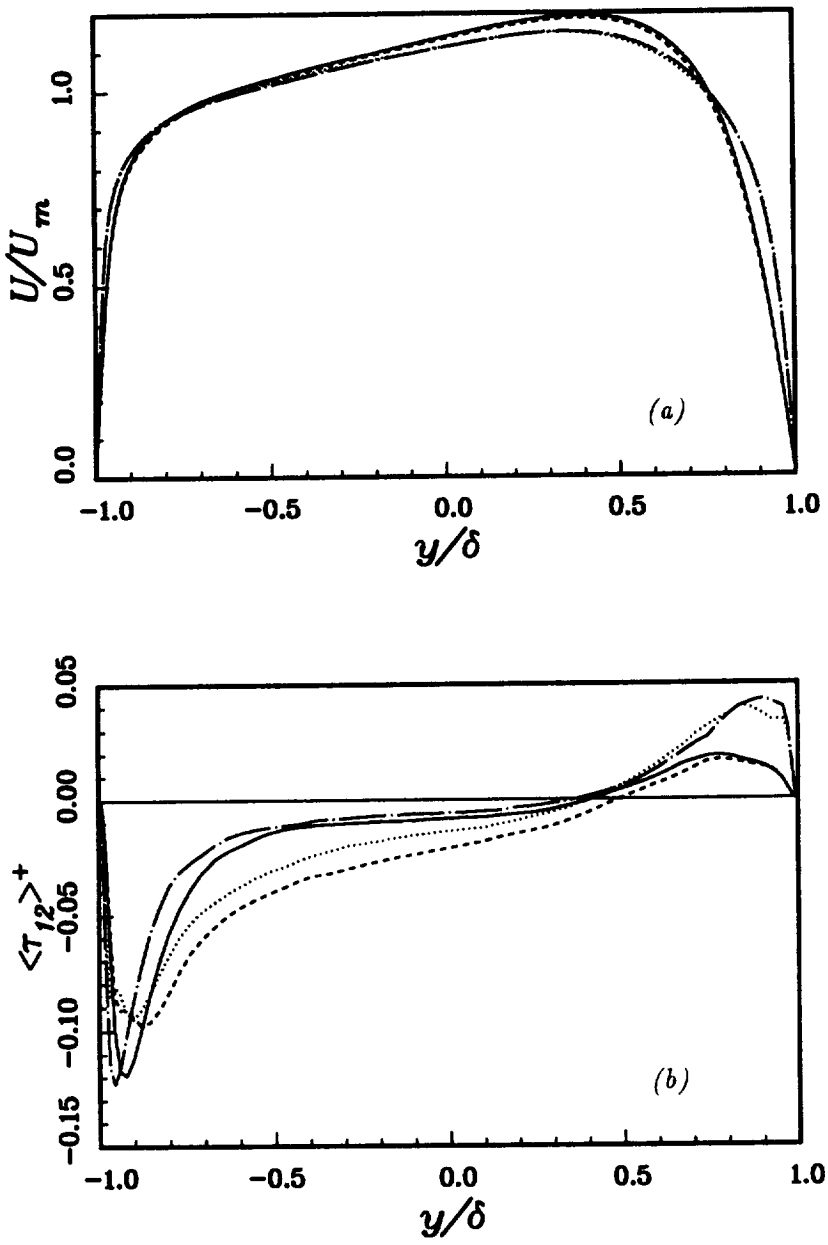

FIGURE 7. The asymmetric vertical distribution of *(a)* mean streamwise velocity and *(b)* mean residual SGS Reynolds stress in the LES of rotating channel flow with $Re_m \approx 5,400$ and 12,000 and using the DA1 model (——— , case 1; —·— , case 3) and, hardly distinguishable in *(a)*, the DA2 model (- - - - , case 2; ····· , case 4) (see Table 1).

REFERENCES

CABOT, W. 1993 Large eddy simulations of time-dependent and buoyancy-driven channel flows. In *CTR Annual Research Briefs 1992*, Center for Turbulence Research, Stanford Univ./NASA Ames Research Center, 45–60.

CABOT, W., HUBICKYJ, O., POLLACK, J. B., CASSEN, P., & CANUTO, V. M. 1990 Direct numerical simulations of turbulent convection: I. Variable gravity and uniform rotation. *Geophys. Astrophys. Fluid Dyn.* **53**, 1–42.

CABOT, W., & MOIN, P. 1993 Large eddy simulation of scalar transport with the dynamic subgrid-scale model. In *Large Eddy Simulation of Complex Engineering and Geophysical Flows*, ed. B. Galperin & S. A. Orszag (Cambridge Univ. Press), ch. 7.

CABOT, W., & POLLACK, J. B. 1992 Direct numerical simulations of turbulent convection: II. Variable gravity and differential rotation. *Geophys. Astrophys. Fluid Dyn.* **64**, 97–133.

GATSKI, T. B., & SPEZIALE, C. G. 1993 On explicit algebraic stress models for complex turbulent flows. *J. Fluid Mech.* **254**, 59–78.

GERMANO, M., PIOMELLI, U., MOIN, P., & CABOT, W. H. 1991 A dynamic subgrid-scale eddy viscosity model. *Phys. Fluids A.* **3**, 1760–1765.

GHOSAL, S., LUND, T. S., & MOIN, P. 1993 A local dynamic model for large eddy simulation. In *CTR Annual Research Briefs 1992*, Center for Turbulence Research, Stanford Univ./NASA Ames Research Center, 3–25.

KIM, J., MOIN, P., & MOSER, R. 1987 Turbulence statistics in fully developed channel flow at low Reynolds number. *J. Fluid Mech.* **177**, 133–166.

LILLY, D. 1992 A proposed modification of the Germano subgrid-scale closure method. *Phys. Fluids A.* **4**, 633–635.

LUND, T. S., & NOVIKOV, E. A. 1993 Parameterization of subgrid-scale stress by the velocity gradient tensor. In *CTR Annual Research Briefs 1992*, Center for Turbulence Research, Stanford Univ./NASA Ames Research Center, 27–43.

MENEVEAU, C., LUND, T. S., & MOIN, P. 1992 Search for subgrid scale parameterization by projection pursuit regression. In *CTR Proceedings of the Summer Program 1992*, Center for Turbulence Research, Stanford Univ./NASA Ames Research Center, 61–81.

MOIN, P., & JIMENÉZ, J. 1993 Large eddy simulation of complex turbulent flows, *AIAA-93-3099*, 24th Fluid Dyn. Conf., Orlando, Florida.

MOIN, P., SQUIRES, K., CABOT, W., & LEE, S. 1991 A dynamic subgrid-scale model for compressible turbulence and scalar transport. *Phys. Fluids A.* **3**, 2746–2757.

SCHUMANN, U. 1991 Subgrid length-scales for large-eddy simulation of stratified turbulence. *Theoret. Comput. Fluid Dyn.* **2**, 279–290.

SCOTTI, A., MENEVEAU, C., & LILLY, D. K. 1993 Generalized Smagorinsky model for anisotropic grids. *Phys. Fluids A.* **5,** 2306–2308.

SPEZIALE, C. G., SARKAR, S., & GATSKI, T. B. 1991 Modelling the pressure-strain correlation of turbulence: an invariant dynamical systems approach. *J. Fluid Mech.* **227,** 245–272.

SQUIRES, K. D., & PIOMELLI, U. 1994 Dynamic modeling of rotating turbulence. In *Turbulent Shear Flows 9,* ed. F. Durst, N. Kasagi, B. E. Launder, F. W. Schmidt & J. H. Whitelaw (Springer-Verlag, Heidelberg), in press.